

A pilot study: 3D stereo photogrammetric image superimposition on to 3D CT scan images – the future of orthognathic surgery

Dr Balvinder Khambay, PhD, FDS RCS, BDS.

Clinical Lecturer in Orthodontics,
Glasgow University School of Dentistry,
378 Sauchiehall Street,
Glasgow,
Scotland, UK.
Fax : +44(0)141 331 2798

Dr Jean-Christophe Nebel, MSc, PhD.

Research Fellow,
3D-Matic Research Laboratory,
University of Glasgow,
Scotland,UK
Fax : +44(0)141 330 3119

Mrs Janet Bowman, BSc, Dip.Math.Stat, PGCE.

Research Assistant,
3D-Matic Research Laboratory,
University of Glasgow,
Scotland,UK
Fax : +44(0)141 330 3119

Mr Frasier Walker, MIMPT,

Principle Maxillofacial Technologist,
Caniesburn Hospital,
Switchback Road,
Bearsden ,
Glasgow,
Scotland, UK
Fax : +44(0)141 211 5652

Professor Donald M Hadley, PhD, FRCR.

Professor in Radiology,
Department of Neuroradiology,
Institute of Neurological Sciences,
Southern General Hospital,
Glasgow,
Scotland, UK
Fax : +44(0)141 445 5273

Dr Ashraf Ayoub, PhD, FDS RCS, FDS RCPS, MDS, BDS.

Senior Clinical Lecturer in Oral & Maxillofacial Surgery
Head of Biotechnology and Craniofacial Research Group,
Glasgow University School of Dentistry,
378 Sauchiehall Street,
Glasgow,
Scotland, UK.
Fax : +44(0)141 211 9834

Please send correspondence to the following address:

Dr. A Ayoub, PhD, FDS RCS, FDS RCPS, MDS, BDS.

Senior Clinical Lecturer in Oral & Maxillofacial Surgery
Head of Biotechnology and Craniofacial Research Group,
Glasgow University School of Dentistry,
378 Sauchiehall Street,
Glasgow,
Scotland, UK.
Fax : +44(0)141 211 9834

A pilot study: 3D stereo photogrammetric image superimposition on to 3D CT scan images – the future of orthognathic surgery

The aim of this study was to register and assess the accuracy of the superimposition method of a 3D soft tissue stereo photogrammetric image (C3D image) and a 3D image of the underlying skeletal tissue acquired by 3D spiral CT (CT image). The study was conducted on a model head, in which an intact human skull was embedded with an overlying latex mask reproducing anatomical features of a human face. Ten artificial radio opaque landmarks were secured onto the surface of the latex mask. A stereo photogrammetric image of the mask and a 3D spiral CT image of the model head were captured. The C3D image and the CT images were registered for superimposition by three different methods; Procrustes superimposition using artificial landmarks, Procrustes analysis using anatomical landmarks, and partial Procrustes analysis using anatomical landmarks and then registration completion by HICP using a specified region of both images. The results showed that Procrustes superimposition using the artificial landmarks and Procrustes analysis using anatomical landmarks produced an error of superimposition in the order of 2mm. Partial Procrustes analysis using anatomical landmarks followed by HICP produced a superimposition accuracy of between 1.25 and 1.5 mm. It was concluded that a stereo photogrammetry and a 3D spiral CT scan image can be superimposed with an accuracy of between 1.25 and 1.5 mm using partial Procrustes analysis based on anatomical landmarks and then registration completion by HICP.

INTRODUCTION

Orthognathic surgery has become a routine procedure over the last three decades for the correction of facial deformity. Pre-operative surgical planning is still a major undertaking, requiring the collaboration of several dental and medical specialties. The most commonly used method of planning is to cut up profile photographs magnified to the same size as the standardized lateral skull radiograph¹. These are then superimposed over the cephalographs. The various portions of soft tissue and underlying bone are moved around to produce the most acceptable result, guided by the known ratios of soft tissue movements to the surgical changes of the underlying bones²⁻⁸. Unfortunately, radiographic and photographic registration and superimposition are approximate because of the distortion inherent in the photograph – the image geometry of the camera that took the photograph and the X-ray machine that took the radiograph are different. The radiographic photographic superimposition is carried out manually using the soft tissue profile and is subject to human error. This method of planning does not lend itself to audit or research, on returning to the plan it is found that the adhesive has degraded and the various portions have separated.

Recently, various computer packages (CASSOS™, SoftEnable Technology, Hong Kong, Dento-Facial Planner™, Dentofacial Software Inc, USA) have become available that have partially replaced the manual method of simulating orthognathic and maxillofacial operations. A digital camera is used to capture the facial profile. Skeletal and dental landmarks are digitised from the lateral cephalograph and superimposed on the facial image. Having achieved a bone-face registration, the surgeon can analysis the face and plan the operation. The software allows automated hard and soft tissue movement using a ratio based on a mathematically derived algorithm. Prior to the final image being available, the prediction

profile is then morphed, a form of computerised smoothing, to provide the patient with a more realistic image of the final predicted surgical outcome.

Two-dimensional planning of a three dimensional subject has obvious flaws, one being the inability of the patient to relate to the post surgical prediction plan. As mentioned previously, 2-D planning is based on a lateral view of the patient, yet very few patients are concerned about their profile, since they rarely see it. The patient's main concerns are often front on facial view problems, since these are experienced everyday in the mirror. To address these problems a truly 3D modality of planning is required.

The basic principles of 3D planning are not that different from 2D planning except that a third dimension of depth is introduced. Obtaining a 3D image of the underlying skeletal tissue is not difficult or new, computerised tomography (CT), magnetic resonance imaging (MRI) can be used as well as 3D reconstruction of axial, sagittal and coronal views.

The problem arises with 3D capturing of the overlying soft tissue and then the accurate and reproducible superimposition of the two tissues to form the on screen 3D model. Many techniques for 3D soft tissue capture are available including, biostereometrics⁹, morphanalysis¹⁰, laser scanning¹¹, 3D digitiser¹², Moire scanning, stereolithography, ultrasonography¹³ and stereo video techniques¹⁴. Each technique is not without its disadvantages, for example, laser scanning takes time to complete (15s) and the eyes need to be closed, morphanalysis uses equipment which is extremely elaborate, expensive and the technique is very complicated and time consuming. Ultrasonography is in its experimental stage and there are major problems with data acquisition, reduction and storage.

The most promising method of soft tissue capture is stereophotogrammetry (C3D image based capture system). This involves the use of a pair of stereo video cameras to capture a stereo image pair of each side of the face, software then allows the construction of a photo-realistic 3D facial model. The model can be rotated, translated and dilated on the computer screen. The concept of 3D planning is also not new; the main focus of recently published work is to modify a soft tissue generic mesh to fit around the patients 3D CT model. During the planning procedure, the bone surface position was changed, accompanied by a corresponding soft tissue coordinate change¹⁵⁻¹⁷. The generic mesh would then be draped with a cartograph of the patients face to produce a texture-mapped image of the face¹⁸. A thorough search of the literature indicates that this whole procedure has not been validated scientifically and may in fact not be clinically accurate. The accuracy of the soft tissue generic mesh to the 3D CT model has not been assessed using this method 3D planning.

In order to register and superimpose data generated by CT scanners and data generated by the C3D image-based capture system, the two sets of data have to be converted into a common 3D file format, which is able to handle 3D models with or without associated texture files. The accuracy with which the two images superimpose will depend on the method of registration used, either Procrustes or ICP (Iterative Closest Point).

Procrustes registration is based on the a prior knowledge of 3D point correspondences, a specially built graphic interface software has been developed to manually set the corresponding 3D landmarks on the 2 models¹⁹. These landmarks are used to solve a rigid body transformation (translation, scaling and rotation) mapping of one model on the other. ICP is a very powerful algorithm; in particular it can handle a reasonable amount of noise. However since it is an iteration of a minimisation problem, the algorithm may converge

towards a local minimum. Generally this was overcome by starting the iteration loop from an approximate registration. The modified version of ICP used was called HICP because it incorporates a weight function²⁰. The main difference from the original ICP algorithm is that HICP considers the outlier problem and instead of using all the closest point pairs obtained in each iteration, each pair is weighted with a weight depending on the distance between them²⁰.

The aim of this study is to develop a process which allows the registration of the 3D geometry of the soft tissue air boundary (acquired by photogrammetry) with a 3D image of the underlying skeletal hard tissue generated by a CT scanner and assess the accuracy of the superimposition method.

MATERIALS AND METHODS

Data acquisition

A Perspex head, in which an intact human skull was embedded, was obtained from the Radiology Department of the Glasgow Dental School, figure 1. A mask was then constructed from Latex on the facial surface of the Perspex head to reproduce the anatomical features of a human face, i.e. eyes, nose, lips, surface colouring and eye brows (Fig 1). Ten landmarks were constructed from self cure acrylic (Orthoresin, Dentsply Ltd, Surrey, UK) and barium sulphate (Baritop Plus granules, Bioglan Laboratories Ltd, Hertordshire). These were then secured on to the surface of the latex mask with cyanoacrylate glue (Sheramega 2000, Shera GmbH & Co, Lemförde). A stereo photogrammetric image of the face and a 3D spiral CT image of the head were captured (Fig 2).

Three-dimensional stereo photogrammetry image acquisition

The three-dimensional images were obtained using a stereo photogrammetry machine (C3D)¹⁴. The technique is based on the use of two pairs of stereo videocameras which are connected to a personal computer. Following calibration, the computer began a sequence of flash and acquisition of video images from both sides of the face. The process took 50 milliseconds. Upon completion of the image capture, the resultant six images (two black and white and one colour image for each side of the face) were saved. Then the data, determined from calibration, were attached to the images of the head. The final image was built using the C3D software and stored as a VRML file (Virtual Reality Modelling Language) – the C3D image.

Three-dimensional spiral CT image acquisition

The three-dimensional images were obtained using a four-slice spiral CT scanner (Marconi MX8000). The rotation time was set at 0.75 seconds with a pitch of 0.625, this gave an effective slice thickness of 1.3mm. A total of 400 slices were captured and stored as DICOM images on a CD-ROM. The 400 DICOM slices were then imported into Amira™ software program (TGS Europe, France) and two 3D CT models built. The first image represented the air / Perspex boundary layer and the second image the skull / Perspex boundary layer. This was achieved by adjusting the threshold during model building in Amira™. These two images were then exported as VRML files with a common co-ordinate system. This produced the VRML 3D CT skin image and the VRML 3D CT skull image (Fig 3).

IMAGE REGISTRATION

The C3D image and the VRML 3D CT skin image was registered for superimposition by three different methods,

1. Procrustes superimposition using the set of 10 artificial landmarks,
2. Procrustes analysis using anatomical landmarks, and
3. A partial Procrustes analysis using anatomical landmarks and then registration completion by HICP using a specified region of the images.

Procrustes superimposition using the set of 10 artificial landmarks

The registration process involved identification of the artificial landmarks on both the C3D image and the VRML 3D CT skin image. The C3D software then superimposed the two images using Procrustes registration (Fig 4).

Procrustes superimposition using anatomical

Ten anatomical landmarks were identified (corners of the eyes, nostrils, mouth, forehead and chin point) on both the C3D image and the VRML 3D CT skin image. Registration was performed using the Procrustes registration.

Procrustes superimposition using anatomical landmarks and then registration completion by HICP

Ten anatomical landmarks were identified (corners of the eyes, nostrils, mouth, forehead and chin point) on both the C3D image and the VRML 3D CT skin image. A partial registration was performed using the Procrustes registration. Then the areas utilised for the HICP registrations were defined on both models. A region around the nose was chosen since it

contained marked feature of the human face (Fig 5). The registration was automatically processed.

ASSESSMENT OF ACCURACY

The accuracy of registration of the C3D image and the VRML 3D CT skin image over one another was evaluated by comparing the distance between the two surfaces. Ideally the two skin surfaces should overlie one another with no space between them. The accuracy of superimposition was assessed by replicating the C3D image from the registered image and using this to create an inner and outer shell i.e. two C3D images either side of the VRML 3D CT skin image. As the distance between the inner and outer shells was reduced an optimum point was reached where by the registered image was neither visible from the front or the back (Fig 6).

The distance between the inner and outer C3D images was set at 4mm, 3mm, 2.5mm and 2mm. The two C3D images and the registered image seen from the front and back of the head were then displayed.

RESULTS

Image registration

Procrustes superimposition using the set of 10 artificial landmarks

Figure 7 shows the superimposition registration based on the 10 artificial landmarks using Procrustes registration.

Procrustes superimposition using anatomical landmarks

Figure 8 shows Procrustes registration based on anatomical landmarks only, together with the profile view of the images.

Procrustes superimposition using anatomical landmarks and then registration completion by HICP

Figure 9 shows Procrustes registration based on anatomical landmarks, the region selected for HICP registration and the final registered meshes.

Assessment of accuracy

Procrustes superimposition using anatomical landmarks

Figure 10(a) and 10(b) shows areas of the VRML 3D CT skin image, in red, that are 2mm or more in front of the C3D image respectively registered by Procrustes only. The more red seen in the images indicates more inaccuracy. Partial Procrustes and HICP registration is more accurate than Procrustes only registration.

Procrustes superimposition using anatomical landmarks and then registration completion by HICP

Figure 11(a) and 11(b) shows areas of the VRML 3D CT skin image, in red, that are 2mm or more in front of the C3D image respectively registered by Procrustes only and partial Procrustes and HICP techniques.

Figure 12 shows the accuracy of the registration process. The more red areas seen in the images indicates more inaccuracy, seen from the front and from the back, whose accuracy is respectively under 2, 1.5, 1.25 and 1mm. The result of this analysis is that most points have an accuracy of at least 1.25 mm

Figure 13 shows the final superimposition model of the C3D image over the VRML 3D CT skull image.

DISCUSSION

In order to register data generated by CT scanners and data generated by the C3D image-based capture system, the two sets of data had to be converted into a common 3D file format, which is able to handle 3D models with or without associated texture file. VRML (Virtual Reality Modelling Language) was chosen for several reasons. First, VRML is the open standard for 3D multimedia and shared virtual worlds on the Internet, which can be read by any Internet browser; therefore VRML data can be visualised without the need of investing in any specialised 3D software. Secondly VRML is the format of the models generated by C3D. Finally the software used for processing the CT scanned data, AmiraTM, has the ability to export files in that format.

Since the models of the skin and the skull are extracted from the CT scanned data with the same coordinate system, the registration need only be performed between the C3D image and the 3D CT skin data to get the three registered models. The registration process was performed in two steps. The first step normalises the position of the C3D and skin data using a Procrustes registration. The second step refines the registration using a modified version of the Iterative Closest Point algorithm (ICP).

The Procrustes registration is based on the a priori knowledge of 3D point correspondences, specially built graphic interface software has been developed to set manually the corresponding 3D landmarks on the 2 models. These landmarks are used to solve a rigid body transformation (translation, scaling and rotation) mapping one model on the other. The relative translation is evaluated by measuring the distance between the centroids of the 2 sets of data. The scale factor is calculated by comparing their sizes; they are estimated by summing the distances between each landmark and the centroid. Finally the relative rotation can be efficiently determined by an established non-iterative method called the Singular

Value Decomposition (SVD) method²¹. If a large number of corresponding landmarks could be set accurately on the 2 images, Procrustes registration could be sufficient to provide an accurate registration between the two 3D images. Previous researches showed that landmarks could be set on textured 3D models with an accuracy of 0.5mm²². However, since the skin data generated by CT scanners is not associated with a texture, landmarks can only be extracted from geometrical features, this limits the number of available landmarks and the accuracy of their selection.

The second step of the registration, which is ICP based, establishes correspondences between data sets by matching points in one data set to the closest points in the other data set. It is an iterative process going through the following steps;

- For each point of mesh A, compute the closest point of mesh B.
- Solving a minimization problem, compute the registration vector.
- Apply the registration and update the position of the points of mesh B.
- Compute the mean square error of the previous iteration and the current iteration.
- Terminate the iteration if the change in mean square error is less than a preset threshold.

As expected an inaccurate registration was produced, with a misalignment of the order of 1 cm, when Procrustes registration was used to superimpose the C3D image and the VRML 3D CT skin image using anatomical markers only.

The superimposition of the two images, using partial Procrustes and HICP registration was much more accurate. Points in the nostril and eyebrow areas however have a poor accuracy as the CT scanner captures the position of the skin behind the eyebrows whereas the C3D

stereophotogrammetry captures the surface defined by the eyebrows. The registration, which was only based on artificial landmarks, was also poor. This can be explained by the fact that the artificial landmarks had very sharp edges, which were smoothed by C3D stereophotogrammetry but not by the CT scanner.

The partial Procrustes and HICP registration analysis has an accuracy of at least 1.25 mm. The inaccuracy of most of the areas can be explained by the known limitations of the C3D technology, eyebrow surface, nostril occlusion, landmark smoothing and distortions at the periphery of the image. Fortunately all these areas are not critical in orthognathic surgery. Therefore the accuracy, which is relevant to our application, is between 1.25 and 1.5 mm. Since the added landmarks added extra differences between the geometries of the CT and C3D surfaces, we can expect that without them the accuracy of the registration would have been better.

CONCLUSIONS

This study has demonstrated the superimposition of two 3-dimensional images obtained by two different modalities, stereo photogrammetry and a 3D spiral CT scan. The aim of the superimposition is to produce a 3D spiral CT scan of a subjects' hard tissue i.e. skull, and over lay this with the subjects soft tissue drape in colour, figure 13. The soft tissue needs to be positioned accurately over the underlying hard tissue. The space between the two would represent the soft tissue thickness. This study addresses these objectives. A registration accuracy of between 1.25 and 1.5 mm at this very early stage is promising. The effect of CT scan slice thickness and the number of slices on the accuracy of superimposition needs to be calculated since the ionising radiation levels need to be kept as low as possible. This research is an exciting step forward for both the clinician and patient, from the point of procedure

planning on a virtual patient to the proposed surgical outcomes in 3-dimensions for the patient.

REFERENCES

1. Henderson D. The assessment and management of bony deformities of the middle and lower face. *Br J Plast Surg* 1974; 27: 287-296.
2. Hohl TH, Epker, BN. Macrogenia: a study of treatment results, with surgical recommendations. *Oral Surg Oral Med Oral Pathol* 1976; 4: 545-567.
3. McDonnell JP, McNeill RW, West RA. Advancement genioplasty: A retrospective cephalometric analysis of osseous and soft tissue change. *J Oral Surg* 1977; 35: 640-647.
4. Robinson SW, Speidel MT, Isaacson RJ, Worms FW. Soft tissue profile change produced by reduction of mandibular prognathism. *Angle Orthod* 1972; 42: 227-235.
5. Suckiel JM, Khon, MW. Soft tissue changes related to the surgical management of mandibular prognathism. *Am J Orthod* 1978; 73: 676-680.
6. Lines PA, Steinhauser EW. Diagnosis and treatment planning in surgical orthodontic therapy. *Am J Orthod* 1974; 66: 378-397.
7. Freihofer HP Jr. Changes in nasal profile after maxillary advancement in cleft and non-cleft patients. *J Maxillofac Surg* 1977; 5: 20-27.

8. Schendel SA, Eisenfeld WH, Bell WH, Epker BN. Superior repositioning of the maxilla: Stability and soft tissue osseous relations. *Am J Orthod* 1976; 70: 663-674.
9. Berkowitz S, Cuzzi J. Biostereometric analysis of surgically corrected abnormal faces. *Am J Orthod* 1977; 72: 526-538.
10. Rabey GP. Current principles of morphanalysis and their implications in oral surgical procedure. *Br J Oral Surg* 1977; 15: 97-109.
11. McCance AM, Moss JP, Wright WR, Linney AD, James DR. A three dimensional soft tissue analysis of 16 skeletal class III patients following bimaxillary surgery. *Br J Oral Maxillofac Surg* 1992; 30: 221-232.
12. Ip HHS, Yin L. Constructing a 3D individualized head model from two orthogonal views. *Vis Comput* 1996, 12: 254-267.
13. Hell B. 3D sonography. *Int J Oral Maxillofac Surg* 1995; 24: 84-89.
14. Ayoub AF, Siebert JP, Wray D, Moos KF. A vision-based three dimensional capture system for maxillofacial assessment and surgical planning. *Br J Oral Maxillofacial Surg* 1998; 36: 353-357.

15. Xia J, Samman N, Yeung RW, Shen SG, Wang D, Ip HH, Tideman H. Three-dimensional virtual reality surgical planning and simulation workbench for orthognathic surgery. *Int J Adult Orthod Orthognath Surg* 2000; 15: 265-282.
16. Xia J, Samman N, Yeung RW, Wang D, Shen SG, Ip HH, Tideman H. Computer-assisted three-dimensional surgical planing and simulation. 3D soft tissue planning and prediction. *Int J Oral Maxillofac Surg* 2000; 29: 250-258.
17. Xia J, Ip HH, Samman N, Wang D, Kot CS, Yeung RW, Tideman H. Computer-assisted three-dimensional surgical planning and simulation: 3D virtual osteotomy. *Int J Oral Maxillofac Surg* 2000; 29: 7-11.
18. Xia J, Wang D, Samman N, Yeung RW, Tideman H. Computer-assisted three-dimensional surgical planning and simulation: 3D color facial model generation. *Int J Oral Maxillofac Surg* 2000; 29: 2-10.
19. Mao Z, Siebert P, Ayoub AF. Development of 3D measuring techniques for the analysis of facial soft tissue change. *Proc Medical Image Computing and Computer-Assisted Intervention 2000, Pittsburgh, USA, 2000.*
20. Haralick RM., Joo H, Lee C, Zhuang X, Vaidya V, Kim M. Pose estimation from corresponding point data. *IEEE Transactions on Systems, Man and Cybernetics.* 1989; 19: 1426-1446.

21. Arun KS, Huang TS, Blostein SD. Least-square fitting of two 3d point sets. IEEE Trans Pattern Anal Machine Intell. 1987; 9: 698-700.

22. Hajeer MY, Millett DT, Ayoub AF, Kerr WJS, Bock M. 3-dimension soft-tissue changes following orthognathic surgery - A preliminary report. 2001; British Orthodontic Conference, Harrogate.

LEGENDS OF FIGURES

Figure 1. (a), (b) show the front and lateral view of the Perspex head, (c), (d) show the profile and front view of the latex mask on the top of the Perspex head.

Figure 2. 3D models generated with and without the C3D texture.

Figure 3. VRML models of the segmented CT data,

(a), (b) Profile and front views of the skull (VRML 3D CT skull image).

(c) Skull with the covering skin.

(d), (e) Models showing the skin surface with the 10 artificial landmarks (VRML 3D CT skin image).

Figure 4. (a) Ten landmarks on the 3D CT scan model (VRML 3D CT skin image).

(b) Ten landmarks on the C3D model (C3D image).

Figure 5. Procrustes registration based on anatomical landmarks and area selected for the HICP registration

Figure 6. 2-Dimensional diagram showing the basis of the local accuracy technique.

Figure 7. Procrustes registration based on 10 artificial landmarks.

Figure 8. Procrustes registration based on anatomical landmarks.

Figure 9. Procrustes registration based on anatomical landmarks and HICP.

Figure 10. (a), (b) are 3D models showing the errors, in red, at 2mm separation between the registered image and its parallel copy using Procrustes analysis for superimposition.

Figure 11. (a), (b) are 3D models showing the errors, in red, at 2mm separation between the registered image and its parallel copy using Procrustes and HICP registration for superimposition.

Figure 12. 3D models showing the errors, in red, at different distances of separation between the registered image and its parallel copy using Procrustes analysis for superimposition at,

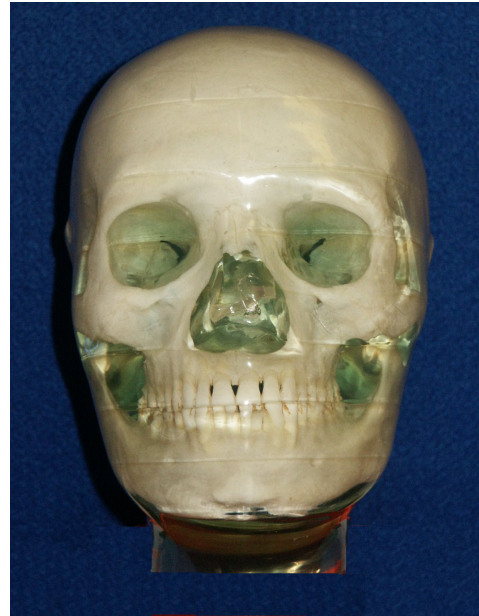
- (a), (e) 2mm separation,
- (b), (f) 1.5 mm separation,
- (c), (g) 1.25 mm separation,
- (d), (h) 1 mm separation,

Figure 13. Superimposition of the C3D stereophotographic image over 3D spiral CT scan image of the skull (VRML 3D CT skull).

FIGURES



(a)



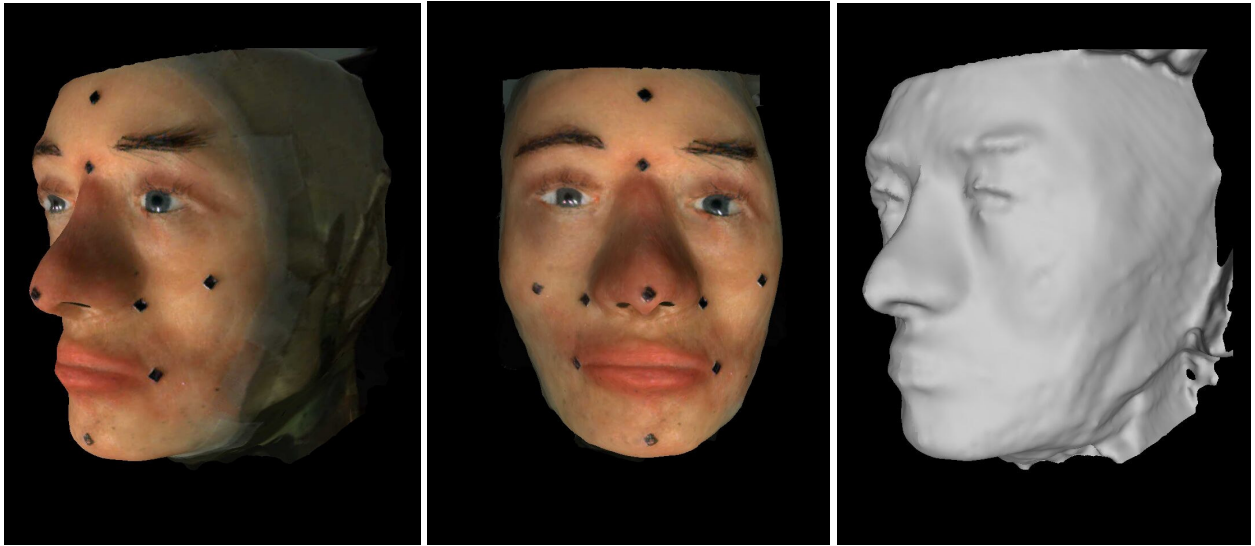
(b)

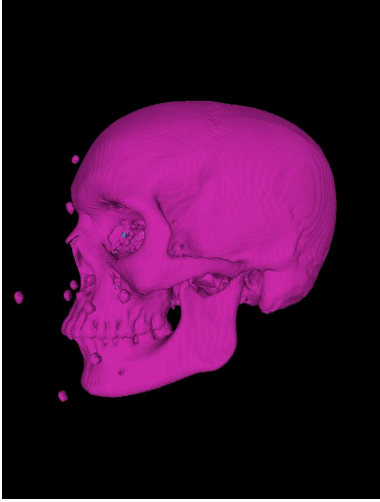


(c)

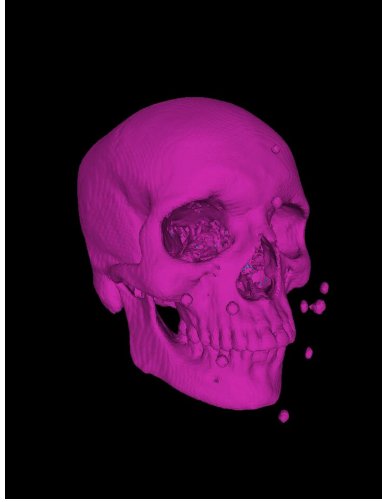


(d)

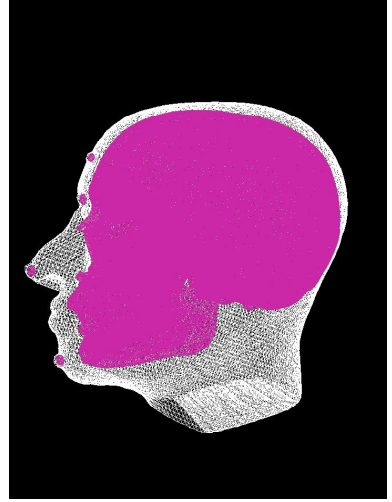




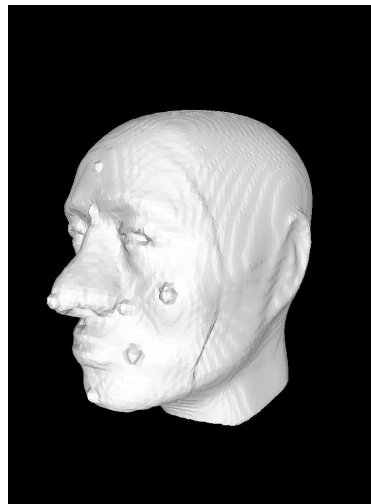
(a)



(b)



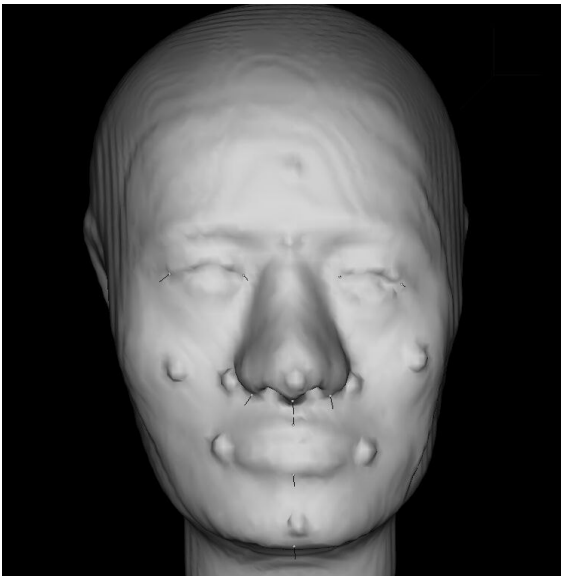
(c)



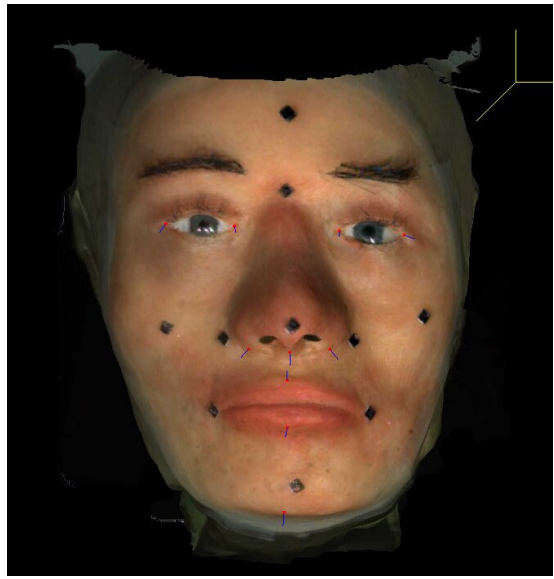
(d)



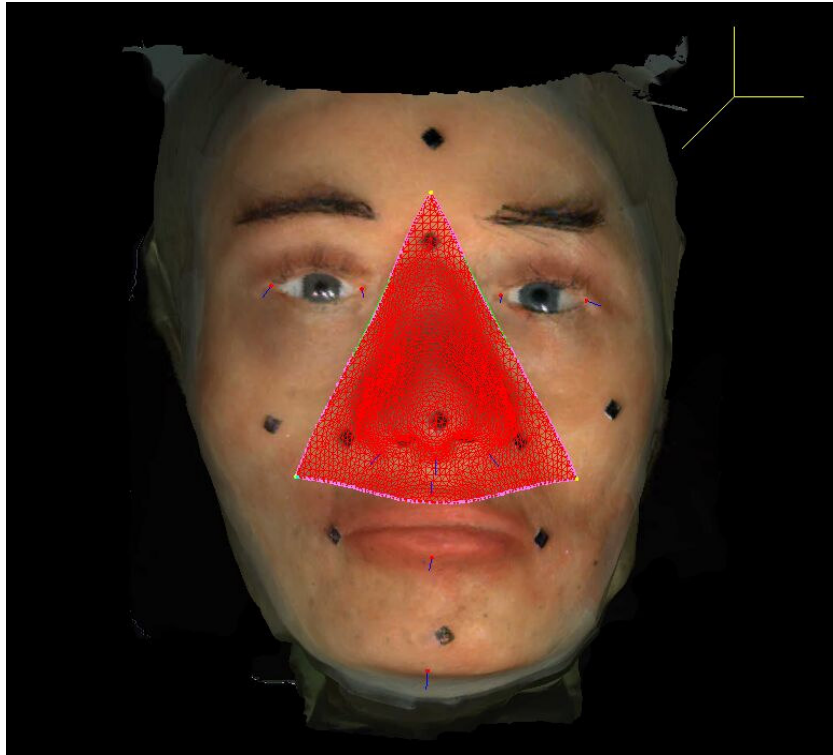
(e)

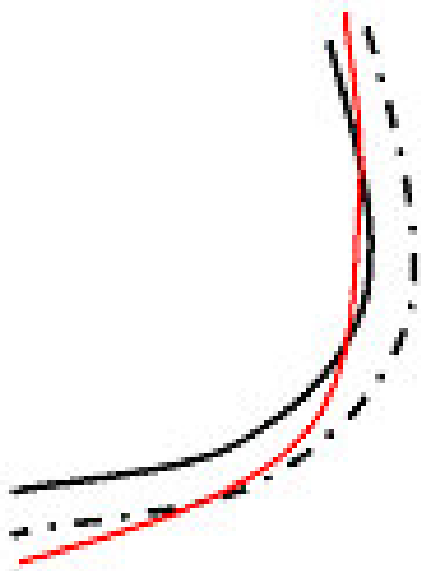


(a)



(b)

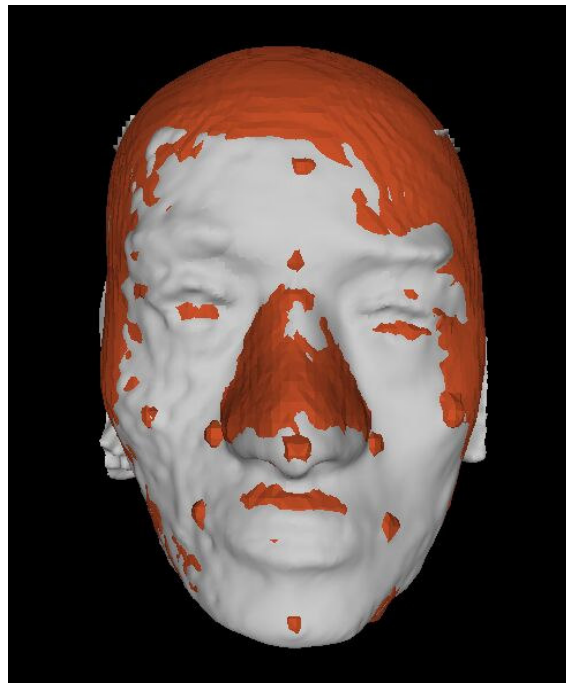


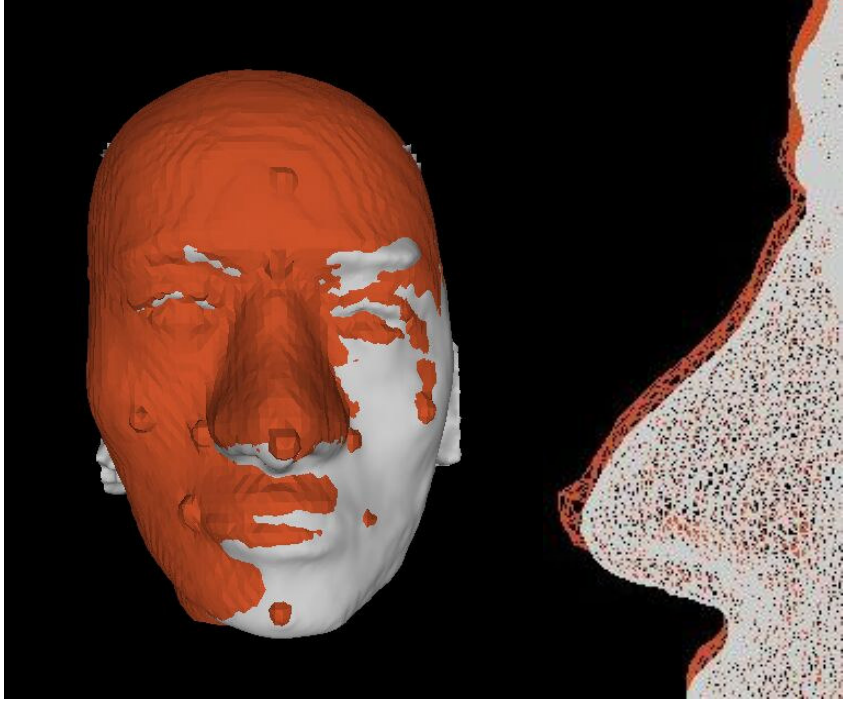


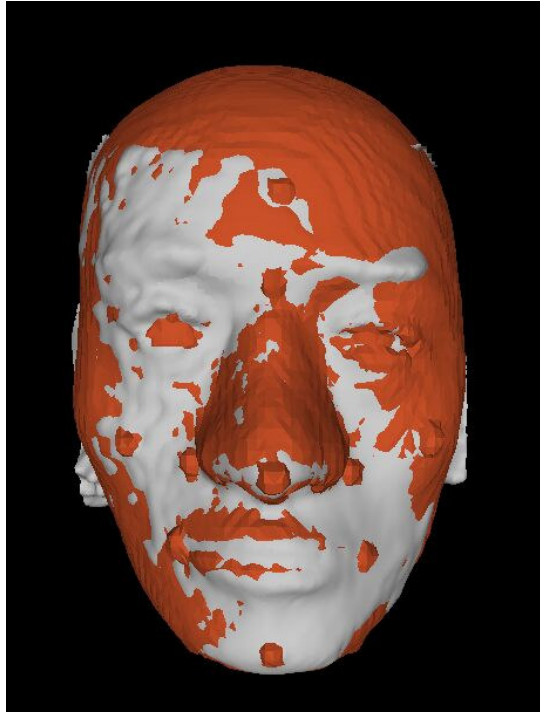
- - - - - Outer shell (C3D image)

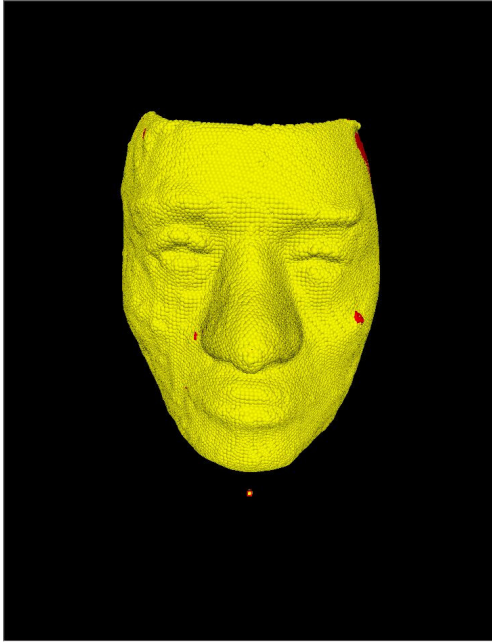
———— Inner shell (C3D image)

———— Registered image

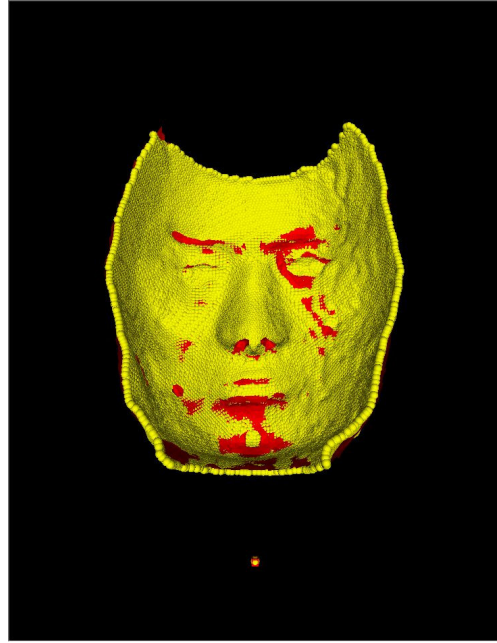




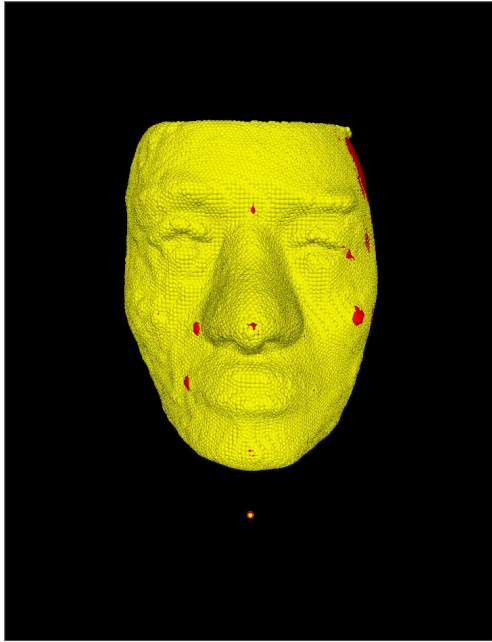




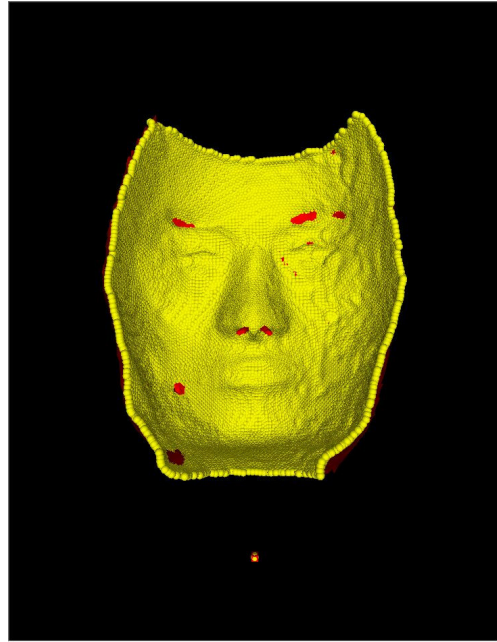
(a)



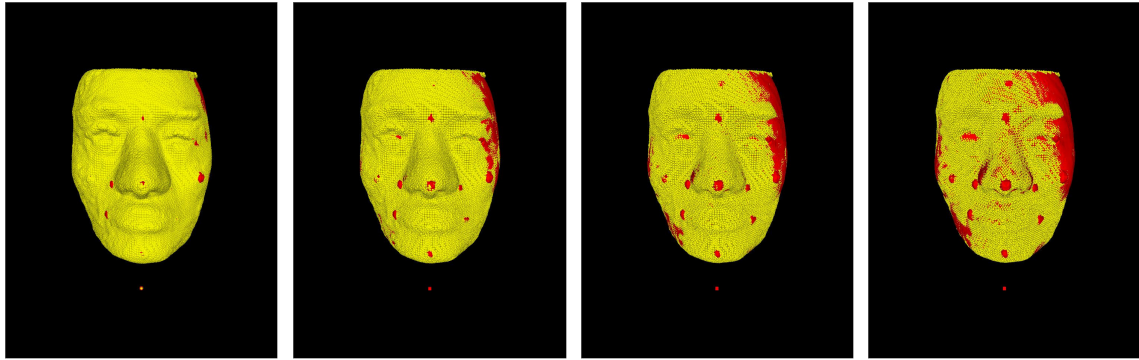
(b)



(a)



(b)

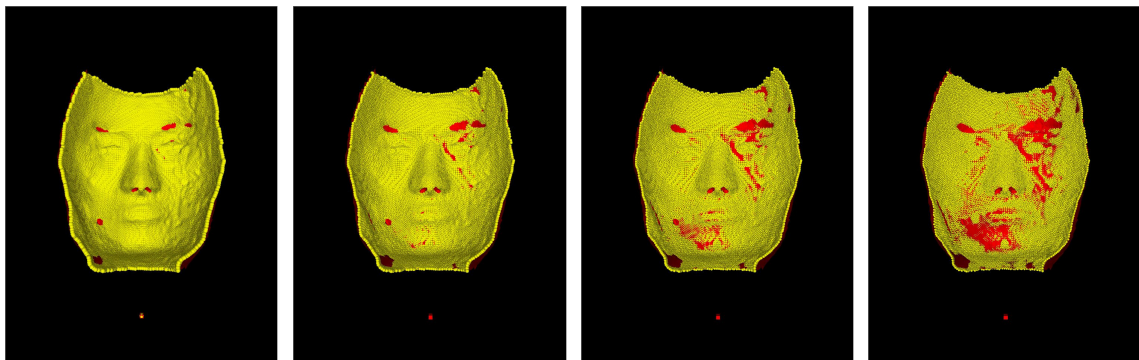


(a)

(b)

(c)

(d)



(e)

(f)

(g)

(h)

